Original Research

Core Ideas

- Plant mucilage and bacterial extracellular polymeric substances (EPS) prevent the breakup of the soil liquid phase.
- Formation of continuous structures buffers soil hydraulic properties.
- The release of viscous polymeric substances represents a universal strategy.

P. Benard, M. Zarebanadkouki, and A. Carminati, Faculty for Biology, Chemistry, and Earth Sciences, Chair of Soil Physics, Univ. of Bayreuth, Universitätsstraße 30, 95447 Bayreuth, Bavaria, Germany; P. Benard, Faculty of Agricultural Sciences, Group of Soil Hydrology, Univ. of Göttingen, Büsgenweg 2, 37077 Göttingen, Lower Saxony, Germany; M. Brax and R. Kaltenbach, Institute for Environmental Sciences, Group of Environmental and Soil Chemistry, Univ. Koblenz-Landau, Fortstraße 7, 76829 Landau, Rhineland-Palatinate, Germany; I. Jerjen and F. Marone, Paul Scherrer Institute, Swiss Light Source, Forschungsstrasse 111, 5232 Villigen, Switzerland; E. Couradeau, Lawrence Berkeley National Lab., Environmental Genomics and Systems Biology, 1 Cyclotron Rd., Berkeley, CA 94720; E. Couradeau, Arizona State Univ., School of Life Sciences, 427 E. Tyler Mall, Tempe, AZ85281; V.J.M.N.L. Felde, Dep. of Soil Science, Univ. of Kassel, Mönchebergstraße 19, 34125 Witzenhausen, Hesse, Germany; A. Kaestner, Paul Scherrer Institute, Lab. for Neutron Scattering and Imaging, Forschungsstrasse 111, 5232 Villigen, Switzerland. *Corresponding author (pascal.benard@uni-bayreuth.de).

Microhydrological Niches in Soils: How Mucilage and EPS Alter the Biophysical Properties of the Rhizosphere and Other Biological Hotspots

Pascal Benard,* Mohsen Zarebanadkouki, Mathilde Brax, Robin Kaltenbach, Iwan Jerjen, Federica Marone, Estelle Couradeau, Vincent J.M.N.L. Felde, Anders Kaestner, and Andrea Carminati

Plant roots and bacteria are capable of buffering erratic fluctuations of water content in their local soil environment by releasing a diverse, highly polymeric blend of substances (e.g. extracellular polymeric substances [EPS] and mucilage). Although this concept is well accepted, the physical mechanisms by which EPS and mucilage interact with the soil matrix and determine the soil water dynamics remain unclear. High-resolution X-ray computed tomography revealed that upon drying in porous media, mucilage (from maize [*Zea mays* L.] roots) and EPS (from intact biocrusts) form filaments and two-dimensional interconnected structures spanning across multiple pores. Unlike water, these mucilage and EPS structures connecting soil particles did not break up upon drying, which is explained by the high viscosity and low surface tension of EPS and mucilage. Measurements of water retention and evaporation with soils mixed with seed mucilage show how these one- and two-dimensional pore-scale structures affect macroscopic hydraulic properties (i.e., they enhance water retention, preserve the continuity of the liquid phase in drying soils, and decrease vapor diffusivity and local drying rates). In conclusion, we propose that the release of viscous polymeric substances and the consequent creation of a network bridging the soil pore space represent a universal strategy of plants and bacteria to engineer their own soil microhydrological niches where stable conditions for life are preserved.

Abbreviations: EPS, extracellular polymeric substances; PSI, Paul Scherrer Institute; SRXTM, synchrotron-based X-ray tomographic microscopy.

Hosting a tremendous biodiversity (Philippot et al., 2013), the soil offers opportunities and numerous challenges to plants and microorganisms therein. Prominent among these challenges are fluctuations in soil water content, which affect growth conditions of plants and soil microorganisms. Since soils are periodically affected by precipitation and evaporation, shifts in hydraulic conditions are mostly inevitable. For example, during severe soil drying, the soil hydraulic conductivity drops and limits the capacity of roots to extract water at the rate required to sustain transpiration. Plants can respond to soil drying by closing stomata, growing deeper roots, changing the root permeability or altering the properties of the soil in their vicinity, the *rhizosphere*. Mucilage secreted by the roots keeps the rhizosphere wet when the soil dries and avoids its quick rewetting after rain or irrigation events (Carminati et al., 2010).

Similar to the effect of mucilage, extracellular polymeric substances (EPS) produced by microorganism buffers fluctuations in soil moisture in hotspots of high biological activity, like the rhizosphere (Kuzyakov and Blagodatskaya, 2015), microbial colonies (Or et al., 2007; Zheng et al., 2018) and biocrusts (Chamizo et al., 2016; Couradeau et al., 2018; Rossi et al., 2018). Biocrusts stand out as an example, arguably the most extended biofilm on the planet (Elbert et al., 2012; Rodriguez-Caballero et al., 2018).

The physicochemical properties of mucilage and EPS highly differ among plant (Naveed et al., 2017) and bacterial (Flemming and Wingender, 2001) species. However, regardless of their diverse composition, mucilage and EPS have some basic traits in common and appear to affect soil hydraulic properties in comparable ways. In this study, we provide experimental evidence and mechanistic explanation of the similarities between mucilage and EPS in shaping the pore-scale spatial configuration of the liquid phase and the consequences on macroscopic hydraulic properties.

Mucilage and EPS have a high polymeric content that confer to mucilage and EPS the hydrogel behavior (Brinker and Scherer, 1990), and as such, they increase the viscosity of the liquid phase (Flemming and Wingender, 2001, 2010; Stoodley et al., 2002; Naveed et al., 2017) and form an interconnected network (Roberson et al., 1993; McCully and Boyer, 1997; Flemming and Wingender, 2010). They act like a porous matrix capable to absorb and hold large quantities of water (Roberson and Firestone, 1992; McCully and Boyer, 1997; Read et al., 1999; Flemming and Wingender, 2001; Segura-Campos et al., 2014). Furthermore, among the exuded compounds, some are powerful surfactants, which decrease the surface tension at the gas–liquid interface (Read et al., 2003; Raaijmakers et al., 2010).

A number of modifications of soil hydraulic properties have been ascribed to mucilage and EPS. An increase in soil water retention was observed within the rhizosphere (Carminati et al., 2010; Moradi et al., 2011) and for seed mucilage (Kroener et al., 2018). Similarly, enhanced water retention was observed for soil inoculated with *Pseudomonas* species previously isolated from soil (Roberson and Firestone, 1992; Volk et al., 2016) and EPS (Chenu, 1993; Rosenzweig et al., 2012), whereas the nondestructive extraction of EPS from biocrust was found to reduce the water-holding capacity of a soil (Adessi et al., 2018).

Due to their high viscosity, mucilage and EPS decrease the saturated soil hydraulic conductivity (Kroener et al., 2014; Volk et al., 2016). The effects on unsaturated conditions are less clear. The decline in hydraulic conductivity with soil water potential was less steep in soils inoculated with biofilm forming bacteria (*Pseudomonas putida*) (Volk et al., 2016). In fine-textured soils, EPS was even shown to increase the unsaturated conductivity (Volk et al., 2016). Along with these modifications, EPS-treated soils (Chenu, 1993; Zheng et al., 2018), soils inoculated with a strain of *Bacillus subtilis* (Zheng et al., 2018), and soil micromodels inoculated with a mucoid strain of *Sinorhizobium meliloti* (Deng et al., 2015) dried slower than unamended control soil. The reduction in drying rates was absent when respective biofilms of *S. meliloti* were studied outside a porous matrix (Deng et al., 2015). Desiccation studies on biofilm forming bacterial strains of *Escherichia coli*, *E. stewartia*, and *Acinetobacter calcoaceticus* in the porous environment of Millipore filters showed a substantially increased survival rate compared with their nonmucoid counterparts (Ophir and Gutnick, 1994).

Despite the consensus on the effects of mucilage and EPS on soil water dynamics (Table 1), the mechanisms of how they interact with the soil matrix and alter soil hydraulic properties are still unknown. The polymer networks of EPS and mucilage can absorb large quantities of water (Roberson and Firestone, 1992; McCully and Boyer, 1997; Read et al., 1999; Flemming and Wingender, 2001), but what forces are responsible to hold this water in soils remains unclear (Flemming, 2011). Extracellular polymeric substances and mucilage can hold water at negative potentials (Chenu, 1993; McCully and Boyer, 1997), but their effect on soil water retention is amplified in fine-textured soils (Kroener et al., 2018), which suggests that additional forces emerge from the interaction between polymers and soil matrix. Similarly, mucilage separated from soil showed no resistance to drying (McCully and Boyer, 1997), and being in a porous system is a prerequisite to allow the polymer network to utilize its full hydraulic capacity (Deng et al., 2015; Kroener et al., 2018). In summary, there is no conclusive theory on the mechanisms by which EPS and mucilage interact with soil and affect their physical properties.

We hypothesize that (i) EPS and mucilage increase viscosity and decrease surface tension of the soil solution and consequently

Table 1. Physical properties of extracellular polymeric substances (EPS) and mucilage and their effects in soil.

Property or effect	Bacterial EPS	Root mucilage	Seed mucilage
	Intrinsic properties		
Increased viscosity and viscoelasticity	Körstgens et al. (2001), Stoodley et al. (2002), Wloka et al. (2004), Shaw et al. (2004), Lieleg et al. (2011)	Read and Gregory (1997), Naveed et al. (2017)	Naveed et al. (2017)
Decreased surface tension	Raaijmakers et al. (2010) and references included	Read and Gregory (1997), Read et al. (2003)	Naveed et al. (2018)
Adsorption of water	Roberson and Firestone (1992), Flemming et al. (2016)	McCully and Boyer (1997), Read et al. (1999)	Segura-Campos et al. (2014)
	Effect on soil hydraulics		
Increased soil water retention	Roberson and Firestone (1992), Chenu (1993), Rosenzweig et al. (2012), Volk et al. (2016)	this study (maize mucilage in glass beads, Supplemental Fig. S1)	Kroener et al. (2018); this study
Slowed down evaporation from soil	Chenu (1993), Flemming (2011), Deng et al. (2015), Zheng et al. (2018), Adessi et al. (2018)	–	this study
Increased relative hydraulic conductivity†	Volk et al. (2016), Zheng et al. (2018)	–	this study

† The relative hydraulic conductivity is defined as the hydraulic conductivity divided by the saturated hydraulic conductivity. This means changes in hydraulic conductivity during drying of soils are eased.

cause the formation of interconnected strands and thin surfaces spanning through multiple pores, and (ii) these pore-scale structures increase water retention, maintain the connectivity of the liquid phase, and decrease gas diffusion on the macroscopic scale. We propose that these mechanisms underlie a universal strategy of plants and bacteria to engineer their local soil physical environment by shaping favorable hydrological niches in soils. We support this statement using existing evidences on EPS and mucilage (Table 1) and a set of novel experiments with porous media (soils of varying textures and glass beads) mixed with maize (*Zea mays* L.) and seed mucilage (*Salvia hispanica* L.), and natural biocrusts.

Conceptual Model Hotspot

As the soil dries, the concentration of polymeric substances in the rhizosphere and other biological hotspots increases. Consequently, the viscosity of the liquid phase increases, and the surface tension decreases, as shown for root mucilage (Read and Gregory, 1997). Changes in viscosity and surface tension affect the spatial configuration of the gas–liquid interface in the pore space. Low surface tension eases the stretching of the gas–liquid interface and decreases its curvature (for a given water potential), according to the Young–Laplace equation:

$$h = \sigma \left(\frac{1}{r_1} + \frac{1}{r_2} \right) \qquad [1]$$

where $h = P_w - P_a$ [Pa] is the difference in pressure between the liquid (P_w) and the gas phase (P_a), σ (mN m^{-1}) is the surface tension of the gas–liquid interface, and r_1 and r_2 (m) are the radii of the curvature of the gas–liquid interface (negative when the radius points toward the liquid phase). Viscosity affects the shape of the liquid bridges between soil particles by avoiding the capillary breakup of the liquid phase (Carminati et al., 2017). The contribution of viscous and surface tension forces on the shape of liquid pendular bridges between particles is elegantly described by the Ohnesorge number, Oh (Ohnesorge, 1936):

$$Oh = \frac{\mu}{\sqrt{\rho \sigma r}} \qquad [2]$$

where μ (Pa s^{-1}) is viscosity, ρ (g m^{-3}) is density, and r (m) is a characteristic length corresponding to the radius of the liquid connection. For Newtonian fluids filaments do not breakup for Oh > 1 (Castrejón-Pita et al., 2012). For mucilage and EPS, the Ohnesorge number increases as the soil progressively dries. When a critical concertation of polymers in the liquid solution is reached, viscosity dominates over inertia and surface tension (Oh >> 1) and the rupture of liquid bridges is prevented. Sattler et al. (2012) showed that even a small concentration of polymer in a liquid solution prevents the breakup of filaments undergoing drying.

Figure 1 shows our conceptual model of the spatial configurations of mucilage and EPS at different contents (dry weight of exudate per weight of soil) after drying in porous media. For low mucilage and EPS contents and large pores, the final shape of arising structures is thin filaments. At intermediate content or at the contact between soil particles, the pendular bridges are cylindrical (Albalasmeh and Ghezzehei, 2014; Benard et al., 2018). They form during soil drying as the gas–liquid interface retreats and the polymers adhering to the soil particle surface are stretched. As the soil dries further, the viscosity increases until a critical point beyond which the polymers cannot be further stretched. At this point, the polymers begin to behave as an additional matrix. The bridges can be drained by air invasion or cavitation. At higher polymer contents, the critical point when neither the network nor the bonds between polymers and particle surfaces can be disrupted is reached at higher volumetric water content when the liquid phase is still connected. In this way, the connectivity of the liquid phase is maintained. We hypothesize that this process results in the formation of two-dimensional interconnected networks that span throughout the porous medium.

Complementary imaging methods are used to support this conceptual model, as well as its implications for macroscopic soil hydraulic properties.

Materials and Methods
Light Microscopy

To illustrate the shape of mucilage structures formed during soil drying, mucilage was mixed with different particles, let dry, and imaged with light microscopy. Samples were prepared according to (Benard et al., 2018). Chia seed mucilage was mixed with a sandy loam at a mucilage content of 4.5 mg g^{-1} (mg dry mucilage g^{-1} soil) (Fig. 2a), with glass beads of 1.7- to 2-mm diameter at a mucilage content of 0.7 mg g^{-1} (Fig. 2b) and fine sand (90% 63–125 μm, 9% 36–63 μm, 1% <36 μm) at a content of 4 mg g^{-1} (Supplemental Fig.
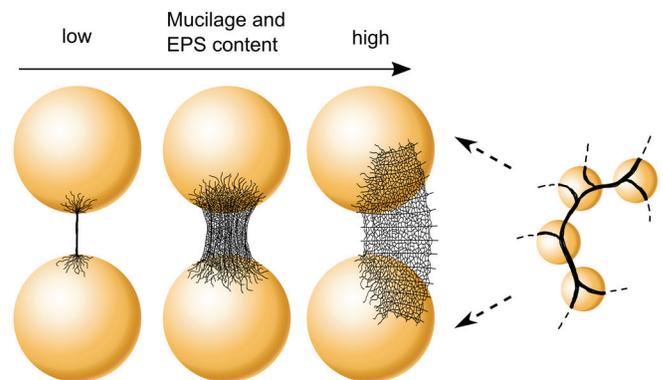

Fig. 1. Spatial configuration of dry mucilage and extracellular polymeric substance (EPS) structures in porous media. Increased viscosity and decreased surface tension of the liquid phase induced by highly polymeric and surface-active substances released by bacteria and plants lead to the formation of characteristic structures in the pore space of drying soil. At low mucilage and EPS contents, isolated threads between particles form in large pores at low water content. Hollow cylinders form in small pores at intermediate mucilage and EPS contents when water is still captured at the inter-particle space. Interconnected two-dimensional structures spanning across multiple pores form at high contents when the liquid phase is still connected (e.g., at considerably high water content).
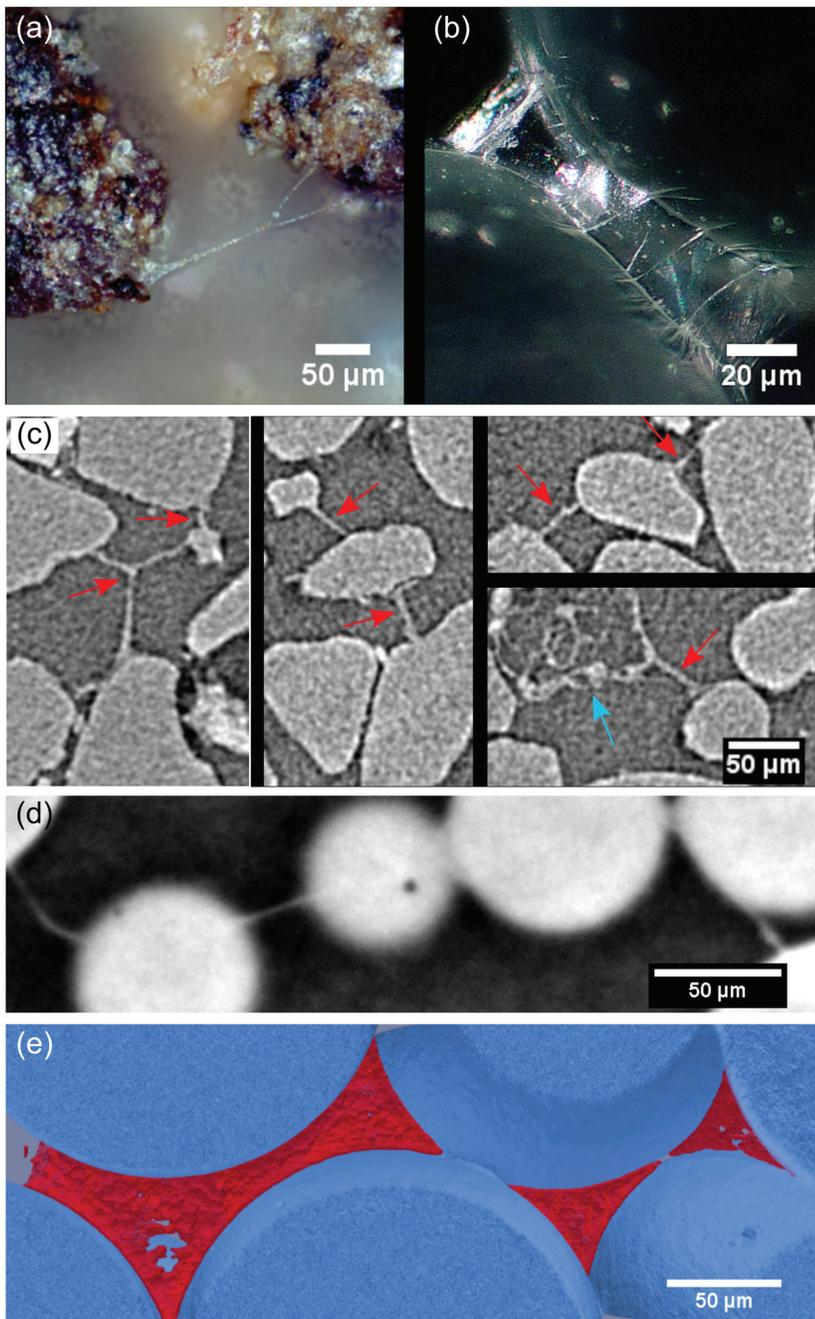
Fig. 2. Examples of polymeric structures formed by mucilage and extracellular polymeric substances (EPS) in porous media: (a) light microscope image of threads of mucilage (mucilage content = 4.5 mg g^{-1} [mg dry mucilage per g of particles]) formed across a large pore during drying; (b) light microscope image of cylinder formed between neighboring glass beads (1.7–2 mm in diameter) at intermediate mucilage content (0.7 mg g^{-1}); (c) two-dimensional EPS-based structures joining quartz grains in intact biocrusts imaged with synchrotron-based X-ray tomographic microscopy (Couradeau et al., 2018), where high EPS content resulted in the formation of characteristic structures (red arrows) comparable with those formed by maize mucilage (the blue arrow marks a cyanobacterial bundle with the EPS sheath surrounding the trichomes of *Microcoleus vaginatus*); (d) cross-section through a synchrotron-based X-ray tomographic microscopy volume of dry maize mucilage structures in glass beads (bright circles) (mucilage content = 8 mg g^{-1}; glass bead diameter = 0.1–0.2 mm); and (e) three-dimensional segmentation of dry mucilage structures (red) from (d) that formed interconnected surfaces of ∼1-μm thickness within the pore space of glass beads (blue). Additional images of mucilage in porous media can be found in Supplemental Fig. S2 to S4.

S4). The sandy loam was collected near Reinhausen (Göttingen, Germany). Total C was 2.0%, total N was 0.17%, and pH was 4.9. The soil texture was distributed as follows: 8.6% clay, 18.5% silt, and 73% sand. The mixtures of particles and mucilage were spread on object slides and left to evaporate at 20°C for 48 h at ambient humidity. Images were acquired with reflected light microscope (Axio Imager 2, Carl Zeiss) equipped with a digital camera (Axiocam 305, software Zen 2 core; Carl Zeiss).

Synchrotron-Based X-Ray Tomographic Microscopy of Maize Mucilage in Glass Beads and Sand

Three-dimensional imaging of maize mucilage in porous media was conducted using synchrotron-based X-ray tomographic microscopy (SRXTM). Experiments were conducted at the TOMCAT (TOmographic Microscopy and Coherent rAdiology experimenTs) beamline (Stampanoni et al., 2006) at the Swiss Light Source at the Paul Scherrer Institute (PSI) in Switzerland. Hydrated mucilage was collected manually from the nodal roots of 10-wk-old field grown maize near Bayreuth, Germany. Mucilage was sucked from nodal roots before they reached the soil on a humid day after a rain event. Mucilage was visible as a blob surrounding the roots. Mucilage concentration was determined by oven drying 50 g of hydrated mucilage. No steps of preprocessing like sterilization were undertaken to minimize alteration of the physical structure and composition of mucilage. Mucilage was frozen after collection, defrosted prior to the experiment, and air dried for 8 h by evaporation. The process was accelerated by a constant air stream above the sample under a fume hood. In this way, the initial concentration of collected mucilage was increased from 8.15 to 15 to 30 mg g^{-1}, respectively (mg of dry mucilage per g of hydrated mucilage) and mixed with glass beads of 0.1 to 0.2 mm in diameter (SWARCO VESTGLAS), achieving a mucilage content of 4 and 8 mg g^{-1} of particles. An exemplary result from a segmented cross-section at 4 mg g^{-1} is shown in Supplemental Fig. S2. Additionally, fine sand (0.125–0.2 mm in diameter) was amended with mucilage from maize in the same way at a content of 8 mg g^{-1} (example cross-sections are shown in Supplemental Fig. S3). Note that Zickenrott et al. (2016) claimed that it is reasonable to expect a mucilage content between 0.05 and 50 mg g^{-1} depending on plant species and conditions. Contents of 4 to 8 mg g^{-1} are therefore at the upper edge of the

plausible range of values. Considering that mucilage content is expected to decrease from the root surface to the bulk soil, the used content is probably representative of the soil very close to the root surface (i.e., at a distance smaller than ∼100 µm). Mixtures were packed in polyvinyl chloride (PVC) cylinders with an inner diameter of 1.5 mm and depth of 4.5 mm. After air drying (at a relative humidity of ∼50%), samples were scanned at 40 keV, with an exposure time of 140 ms per projection, pixel size of 0.325 µm, and field of view of 2560 by 2160 pixels. The sample-detector distance was 24.5 mm. We acquired 1501 projections equiangularly spaced over 180°. The acquired projection images were flat- and dark-field corrected before phase retrieval according to Paganin et al. (2002). Sinograms were then reconstructed to axial tomographic slices using highly optimized routines based on the Fourier transform method (Marone et al., 2017). After reconstruction of three-dimensional volumetric data, particles, air-filled pores, and mucilage structures were segmented using a thresholding technique in MATLAB (The MathWorks, 2017). A series of opening and closing filters followed by a morphological reconstruction algorithm and application of a local threshold were performed to increase the contrast and subsequent segmentation of objects.

Synchrotron-Based X-Ray Tomographic Microscopy of Biocrust from Moab

As an example of two-dimensional EPS structures formed in a natural system, SRXTM of biocrust from Moab, UT, was performed at the Beamline 8.3.2 of the Advanced Light Source (ALS) at Lawrence Berkeley National Laboratory in California. X-ray energy was 25.7 keV and 1025 projections were acquired for the scan at 0.25-s acquisition time. The resulting voxel edge length was 1.3 µm. A more detailed description of the procedure can be found elsewhere (Couradeau et al., 2018).

Soil Water Retention, Hydraulic Conductivity, and Evaporation Measurements

To study the impact of pore-scale spatial configuration of mucilage and EPS on macroscopic soil hydraulic properties, we conducted an evaporation experiment that provides the water retention curve, the unsaturated hydraulic conductivity and evaporative fluxes (Schindler et al., 2010). This method is implemented in Hyprop (METER Group). A cylinder with inner diameter of 8 cm and height of 5 cm was filled with wet sandy loam (see description of light microscopy for details, bulk density of 1.57 g cm^{-3}) and pre-saturated by capillary rise. Note that the porosity of mucilage-amended soil was slightly higher due to its swelling behavior, which explains the offset in initial water content. Evaporation rate and soil matric potentials were recorded during soil drying at a temperature of 25°C. The measurements were repeated two times for a soil mixed with mucilage extracted from chia seeds at a content of 2.5 mg g^{-1} and a control soil pre-saturated with deionized water. As a model of root exuded mucilage, we used chia seed mucilage, which can be extracted in sufficient amounts, and its physical properties and impacts on soil hydraulic properties

are comparable with those of root-exuded mucilage (e.g., maize; Naveed et al., 2017). The procedure of mucilage extraction is described elsewhere (Kroener et al., 2018). To parameterize the hydraulic properties of the mucilage-amended soil and the control soil, data of fluxes and matric potentials were used to simulate water flow during soil drying. Flow of water was simulated by solving the Richards equation using a fully implicit Euler time discretization and a centered finite difference space discretization scheme in MATLAB (Celia and Binning, 1992). Soil water retention and hydraulic conductivity curves were parametrized according to the Peters–Durner–Iden (PDI) model (Peters et al., 2015) and were inversely adjusted to best reproduce the recorded matric potentials and average soil water content.

The evaporation rate of deionized water and mucilage (apart from soil) was monitored at 25°C using the scales of the Hyprop setup. Mucilage extracted from chia seeds, as described in the paragraph above, and deionized water were used. Sets of three replicates of cylindrical containers with an inner diameter of 4 cm and a depth of 1 cm were filled with water and mucilage, respectively, and evaporative fluxes were derived from changes in weight over time. The initial concentration of extracted mucilage was 0.56 g of dry matter per 100 g of liquid solution.

Evaporation from Mucilage-Amended Soil: Neutron Radiography

Neutron radiography allows quantitative imaging of water in soils (Lehmann and Wagner, 2010). Here, it was used to investigate the effect of mucilage on soil moisture distribution during water evaporation from soils. The measurements were performed at the ICON (Imaging with COld Neutrons) beamline at the PSI, Villigen, Switzerland. Containers of size 10 by 1 by 1 cm were filled with a sandy loam (see description of light microscopy for details) amended with chia seed mucilage at a mucilage content of 4.5 mg g^{-1}. As a control, we used the same soil without mucilage addition. To achieve the same porosity, the containers were filled with wet soil (mixed with hydrated mucilage or water) to achieve a bulk density of 1.57 g cm^{-3}. Subsequently, the soil was saturated by capillary rise for 48 h. Porosity of mucilage-amended soil was slightly higher, which explains the offset in initial water content. A time series of neutron radiographs was acquired to monitor water redistribution over a drying period of 4 d. Details on neutron radiography technique and image processing can be found elsewhere (Carminati et al., 2010).

Results and Discussion

Imaging of EPS and Mucilage in Soils

Evidence supporting the conceptual model (Fig. 1) for seed mucilage-forming filaments and hollow cylinders is shown in Fig. 2a and 2b. Similar structures are created by *Bacillus subtilis* in sand (Zheng et al., 2018).

The two-dimensional thin layers predicted for high polymer concentrations are shown for dry maize mucilage in glass beads

(Fig. 2d and 2e) scanned with synchrotron X-ray tomography. A thin layer of dry mucilage forms a continuous surface spanning across multiple pores at a mucilage content of 8 mg g^{-1}. Note that structures of similar extent were also observed at a mucilage content of 4 mg g^{-1}, and an exemplary result of a segmented cross-section is shown in Supplemental Fig. S2.

Similar filaments and surfaces are visible also in biocrusts. Figure 2c shows examples of the two-dimensional thin surfaces visible in the pore space of soil biocrust collected in Moab, UT (Couradeau et al., 2018), observed with synchrotron based X-ray tomography. The similarity between the observed structures of plant and bacterial origin is striking. Their thickness, as well as their vertical extent, is comparable (e.g., Fig. 2). Note that these structures might not be solely composed of EPS. However, the high biological activity and EPS amount found in soil biocrust support the hypothesis that the observed structures are mostly composed of EPS.

Water Retention and Hydraulic Conductivity

Drying of mucilage and EPS in porous media leads to the formation of a matrix that affects the retention and connectivity of water (e.g., Fig. 3–4). The enhanced water retention in soils is partly explained by the hygroscopic properties of mucilage, but the interaction of mucilage with porous media can further increase this effect.

When mucilage and EPS dry outside a porous medium, the decreasing capillary pressure leads to the collapse of their polymer network (Brinker and Scherer, 1990). The situation is different when mucilage and EPS dry within a porous medium. Their high viscosity and entanglement with the soil solid particles prevent their complete collapse, leading to the formation of aforementioned filaments and thin layers that act as a new matrix (Fig. 2–3). Water is retained within the matrix, either inside isolated hollow cylinders (Fig. 2b) or between interconnected gas–liquid interfaces where a dense and stiff layer of polymers prevents air invasion (Fig. 2c–2e). The emerging matrix creates an additional matric potential that can further enhance the retention of water in soils. To what extent the emerging matrix augments the water retention of soils is still not known. Kroener et al. (2018) reported greater water retention of mucilage in fine- than in coarse-textured soils. The pronounced water retention in fine-textured soils can be explained by the higher specific surface area of these soils and the amplified entanglement of polymers with the soil particles, which favors the formation of the polymer matrix across the pore space. This result supports our hypothesis that the emerging polymer matrix is capable of increasing water retention in soils.

Besides enhancing water retention (Fig. 3a and 4a), the high viscosity and low surface tension of mucilage maintain the connectivity of the liquid phase in drying soils (Fig. 3b), which has an important effect on the unsaturated soil hydraulic conductivity. The hydraulic conductivity of a sandy loam (see description of light microscopy for details) amended with seed mucilage did not decline as much as that of the control soil, and at water potentials lower than -10^4 cm (equivalent to -1 MPa), it is even higher (Fig. 4b). The latter is explained by the maintained connectivity of the liquid phase during drying, which enables film flow at low water potentials. This result shows that the maintained connectivity of the liquid phase during drying counteracts the expected decrease in permeability caused by the shrinkage of the polymer matrix (Kroener et al., 2018).

Note that the relative importance of these counteracting processes (i.e., the enhanced retention and connectivity vs. the increasing viscosity) on the unsaturated conductivity is soil texture dependent, as seen in previous studies (Volk et al., 2016; Zheng et al., 2018).
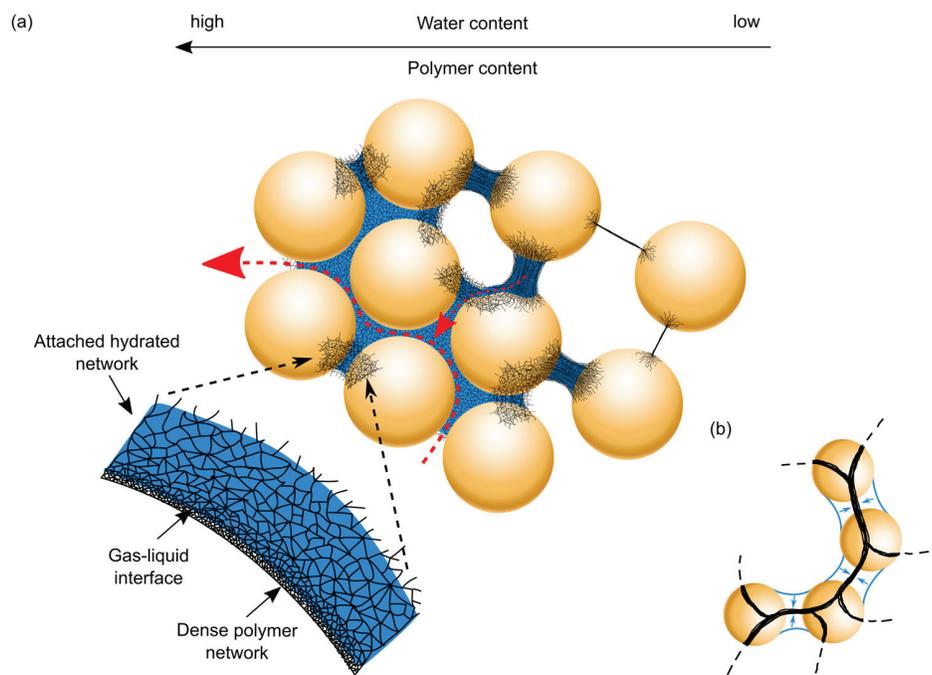

Fig. 3. Configuration of the liquid phase in soils containing extracellular polymeric substances (EPS) or mucilage. (a) In this illustration, the concentration of EPS or mucilage increases from the right to the left. During drying, the gas–liquid interface retreats and the polymers accumulate at this interface. At low polymer contents, the gas–liquid interface retreats but the liquid phase is not broken, which results in the formation of thin threads. At higher polymer contents, the gas–liquid interface becomes stiffer because of the entanglement of the polymers among themselves and with the soil particles. As drying progresses, the gas–liquid interface can no longer be stretched and starts to act as an additional matrix. Together with the hygroscopic nature of the polymers, this leads to an amplified soil water retention. Besides increasing the water retention, the polymer network preserves the continuity of the liquid phase (the flow of water is illustrated by the dashed red arrows). (b) The liquid phase remains connected during drying, with the liquid converging into the two-dimensional surfaces imaged in Fig. 2c to 2e. This induces a shift toward higher hydraulic conductivity in dry soils.
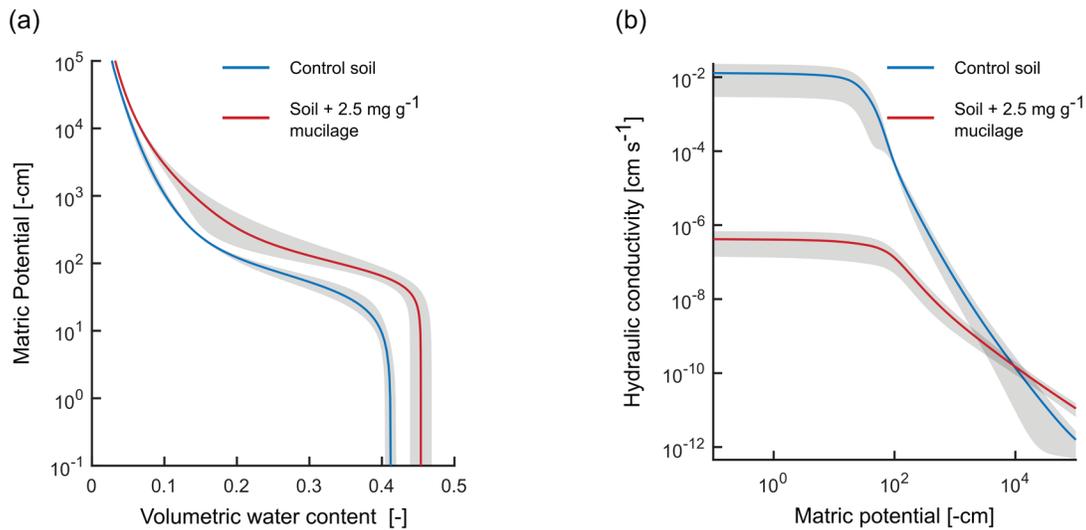
Fig. 4. Water retention and hydraulic conductivity of sandy loam and sandy loam amended with seed mucilage: (a) water retention and (b) hydraulic conductivity curve of a sandy loam without (blue) and amended with seed mucilage (mucilage content = 2.5 mg g^{-1}, *Salvia hispanica*, red). Solid lines indicate the mean of three replicates, and gray areas indicate the 95% confidence interval of three replicates.

Evaporation from Soils

Figure 5 displays the evaporative fluxes in water, mucilage, and in a sandy loam (see description of light microscopy for details) mixed with varying amount of mucilage from chia seeds. Mucilage strongly reduced the evaporative fluxes in soil. However, the evaporation rates in water and mucilage (outside the soil) were similar. For soils embedded with EPS, a similar deceleration in soil drying was explained by the decrease in both saturated hydraulic conductivity and surface tension, which limit capillary rise, causing a discrepancy between evaporative flow and capillary flow and the consequent breakup of the liquid phase. This point marks the transition from Stage I (evaporation from the soil surface) to Stage II of

soil drying (Zheng et al., 2018), when evaporation is reduced and controlled by vapor diffusion through the pore space (Lehmann et al., 2008).

We propose that the suppression of evaporation in soils amended with EPS and mucilage is further reduced by the thin layers shown in Fig. 2c to 2e. These structures are fostered by the decrease in saturated hydraulic conductivity, which does not allow capillary flow to match the evaporative rate, causing a fast drying of the soil surface (Fig. 6a). Once these structures are formed, they limit the diffusion of vapor through the soil. Figure 6b shows a timeline of neutron radiographs of two soil columns, one amended with chia seed mucilage at a content of 4.5 mg g^{-1} (bottom) and
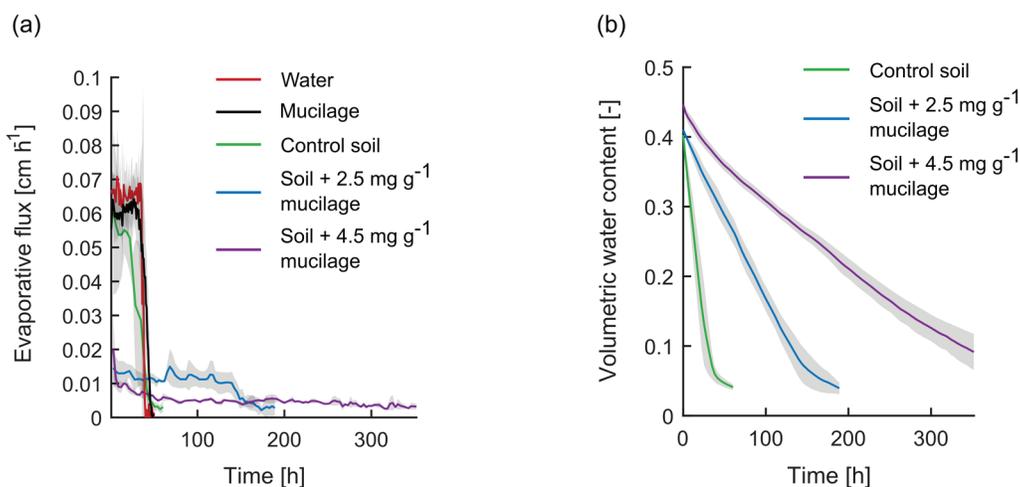

Fig. 5. Evaporative flux and decrease in water content for water and mucilage separate and mixed with soil. Mucilage within the pore space of sandy loam results in a marked decrease in evaporative flux and a delay in soil drying: (a) evaporative flux from free water (red), mucilage (black), control soil saturated with water (green), and soil treated with mucilage (mucilage content = 2.5 mg g^{-1} [blue], mucilage content = 4.5 mg g^{-1} [purple], *Salvia hispanica*); and (b) decrease in water content from an evaporation experiment in soil amended with mucilage (control soil [green], mucilage content = 2.5 mg g^{-1} [blue], mucilage content = 4.5 mg g^{-1} [purple], *Salvia hispanica*). Solid lines indicate the mean of three measurements, and gray areas indicate the 95% confidence interval of three replicates.
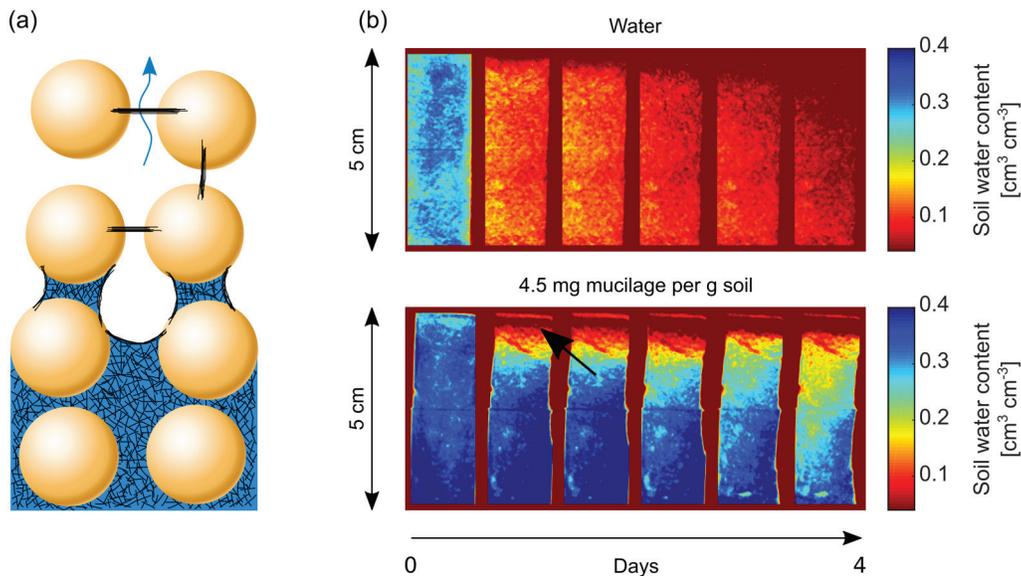
Fig. 6. Delay in evaporation induced by the formation of dense polymer layers in the soil pore space: (a) dense layers of desiccated polymers limit the evaporative flux of water vapor through the soil and delay its drying; and (b) neutron radiographs of two soil columns saturated with water (top) and amended with mucilage (mucilage content = 4.5 mg g^{-1}, *Salvia hispanica*, bottom) over the course of 4 d. The uppermost layer (black arrow) of the mucilage-treated soil dried comparably quickly, whereas the underlying pore space remained wet.

one control initially saturated with water (top). The uppermost layer of the mucilage-amended sample quickly dried (black arrow), confirming our interpretation of the process.

Since evaporation from mucilage and EPS (Deng et al., 2015) (outside the geometry of a porous matrix) showed no substantial resistance to drying (e.g., Fig. 5a), the water adsorptive potential of the polymer network is of secondary importance in slowing down soil drying. Instead, the thin layers of desiccated mucilage and EPS forming in porous media are the main reason for the suppression of evaporation from drying soils. Note that besides reducing vapor diffusion, the dry polymeric layers are also expected to limit the diffusion of O$_2$ and other gases, with additional potential consequences for plant and soil processes.

The suppressed evaporation is of particular importance for the hydrology of biocrust. Due to their global extent and role in nutrient cycling, biocrusts are an important example of soil regions with high EPS content. The formation of thin surfaces spanning throughout the pore space of biocrusts reduces evaporative fluxes, maintains the soil moisture, and preserves the continuity of the liquid phase. By slowing down the desiccation, the network of thin surfaces could be beneficial for the microbial community by granting it more time to perform the metabolic shift underlying the transition to an inactive, dry period.

◆ Conclusions

This study provides a key missing link between pore-scale mechanisms and macroscopic alterations of soil hydraulic properties and soil water dynamics induced by mucilage and EPS. The highly polymeric blend of substances composing mucilage and EPS forms a network, increases the viscosity of the soil solution,

and lowers its surface tension. As soils dry, the polymer network is stretched and its high viscosity and entanglement with soil particles result in the formation of interconnected one- and two-dimensional structures. The formed matrix increases the water retention and liquid connectivity in porous media and decreases the diffusion of gases. The formation of thin layers spanning through the soil pore space decreases vapor diffusion.

The interactions between the highly polymeric blend of mucilage and EPS with the soil pore space have not been recognized so far. The impact on soil hydraulic properties was mostly ascribed to the intrinsic properties of these blends. Our experimental results provided first evidence that the spatial configuration of the liquid phase and the interactions of mucilage and EPS with the soil matrix need to be considered to grasp their impact on soil hydraulics and water dynamics.

The mechanisms described here have been based on model systems (mucilage mixed with repacked soil particles of varying texture), and further research is needed to prove the relevance of mucilage structure formation in the rhizosphere of varying plant species and soil types and their putative function on water and solute uptake. The biocrust images prove that two-dimensional structures reaching across multiple pores can be found in intact soil samples with high biological activity. We propose that the formation of a viscous polymer matrix takes place in biological hotspots in soils, such as the rhizosphere and microbial colonies, and their consequences are manifold. The enhanced continuity of the liquid phase maintains the flow of water and diffusion of solutes required by plants and microorganisms. For plants exposed to severe soil drying, this would enable the root system to sustain transpiration and nutrient uptake. The suppressed evaporation can be particularly important for bacterial colonies (such as in biocrust), slowing down the local

soil drying and reducing pace and likeliness of severe desiccation. In such biological hotspots, the creation of these microhydrological niches might be critical to support life in soil. We propose that the edaphic way of life might have selected common strategies across taxa to tackle the challenges of highly variable soil water dynamics.

In summary, this study explains basic biophysical mechanisms supporting the conditions for life in soils. Countless experiments and observations prove that bacteria and plants are capable of engineering soil hydraulic properties to their advantage. The magnitude and relevance are manifold, as well as the composition of the polymeric blends released, but the underlying mechanisms of how bacteria and plant roots create their microhydrological niches appear universal.

Supplemental Material

The supplemental material displays the positive effect of maize mucilage on water retention in glass beads quantified with neutron radiography and images of dry maize mucilage structures in different textures.

Data Availability

The datasets generated and material used in and/or analyzed during the current study are available from the corresponding author on reasonable request.

References

Adessi, A., R. Cruz de Carvalho, R. De Philippis, C. Branquinho, and J. Marques da Silva. 2018. Microbial extracellular polymeric substances improve water retention in dryland biological soil crusts. Soil Biol. Biochem. 116:67–69. doi:10.1016/j.soilbio.2017.10.002

Albalasmeh, A.A., and T.A. Ghezzehei. 2014. Interplay between soil drying and root exudation in rhizosheath development. Plant Soil 374:739–751. doi:10.1007/s11104-013-1910-y

Benard, P., M. Zarebanadkouki, C. Hedwig, M. Holz, M.A. Ahmed, and A. Carminati. 2018. Pore-scale distribution of mucilage affecting water repellency in the rhizosphere. Vadose Zone J. 17:170013. doi:10.2136/vzj2017.01.0013.

Brinker, C.J., and G.W. Scherer. 1990. Sol-gel science: The physics and chemistry of sol-gel processing. Acad. Press, Boston, MA.

Carminati, A., P. Benard, M.A. Ahmed, and M. Zarebanadkouki. 2017. Liquid bridges at the root–soil interface. Plant Soil 417:1–15. doi:10.1007/s11104-017-3227-8

Carminati, A., A.B. Moradi, D. Vetterlein, P. Vontobel, E. Lehmann, U. Weller, et al. 2010. Dynamics of soil water content in the rhizosphere. Plant Soil 332:163–176. doi:10.1007/s11104-010-0283-8

Castrejón-Pita, A.A., J.R. Castrejón-Pita, and I.M. Hutchings. 2012. Breakup of liquid filaments. Phys. Rev. Lett. 108:074506. doi:10.1103/PhysRevLett.108.074506

Celia, M.A., and P. Binning. 1992. A mass conservative numerical solution for two-phase flow in porous media with application to unsaturated flow. Water Resour. Res. 28:2819–2828. doi:10.1029/92WR01488

Chamizo, S., Y. Cantón, E. Rodríguez-Caballero, and F. Domingo. 2016. Biocrusts positively affect the soil water balance in semiarid ecosystems: The role of biocrusts in the local water balance. Ecohydrology 9:1208–1221. doi:10.1002/eco.1719

Chenu, C. 1993. Clay– or sand–polysaccharide associations as models for the interface between micro-organisms and soil: Water related properties and microstructure. Geoderma 56:143–156. doi:10.1016/0016-7061(93)90106-U

Couradeau, E., V.J.M.N.L. Felde, D. Parkinson, D. Uteau, A. Rochet, C. Cuellar, et al. 2018. In situ X-ray tomography imaging of soil water and cyanobacteria from biological soil crusts undergoing desiccation. Front. Environ. Sci. 6:65. doi:10.3389/fenvs.2018.00065

Deng, J., E.P. Orner, J.F. Chau, E.M. Anderson, A.L. Kadilak, R.L. Rubinstein, et al. 2015. Synergistic effects of soil microstructure and bacterial EPS on drying rate in emulated soil micromodels. Soil Biol. Biochem. 83:116–124. doi:10.1016/j.soilbio.2014.12.006

Elbert, W., B. Weber, S. Burrows, J. Steinkamp, B. Büdel, M.O. Andreae, and U. Pöschl. 2012. Contribution of cryptogamic covers to the global cycles of carbon and nitrogen. Nat. Geosci. 5:459–462. doi:10.1038/ngeo1486

Flemming, H.-C. 2011. The perfect slime. Colloids Surf. B 86:251–259. doi:10.1016/j.colsurfb.2011.04.025

Flemming, H.-C., and J. Wingender. 2001. Relevance of microbial extracellular polymeric substances (EPSs): I. Structural and ecological aspects. Water Sci. Technol. 43(6):1–8. doi:10.2166/wst.2001.0326

Flemming, H.-C., and J. Wingender. 2010. The biofilm matrix. Nat. Rev. Microbiol. 8:623–633. doi:10.1038/nrmicro2415

Flemming, H.-C., J. Wingender, U. Szewzyk, P. Steinberg, S.A. Rice, and S. Kjelleberg. 2016. Biofilms: An emergent form of bacterial life. Nat. Rev. Microbiol. 14:563–575. doi:10.1038/nrmicro.2016.94

Körstgens, V., H.C. Flemming, J. Wingender, and W. Borchard. 2001. Influence of calcium ions on the mechanical properties of a model biofilm of mucoid *Pseudomonas aeruginosa*. Water Sci. Technol. 43:49–57. doi:10.2166/wst.2001.0338

Kroener, E., M. Holz, M. Zarebanadkouki, M. Ahmed, and A. Carminati. 2018. Effects of mucilage on rhizosphere hydraulic functions depend on soil particle size. Vadose Zone J. 17:170056. doi:10.2136/vzj2017.03.0056.

Kroener, E., M. Zarebanadkouki, A. Kaestner, and A. Carminati. 2014. Nonequilibrium water dynamics in the rhizosphere: How mucilage affects water flow in soils. Water Resour. Res. 50:6479–6495. doi:10.1002/2013WR014756

Kuzyakov, Y., and E. Blagodatskaya. 2015. Microbial hotspots and hot moments in soil: Concept & review. Soil Biol. Biochem. 83:184–199. doi:10.1016/j.soilbio.2015.01.025

Lehmann, P., S. Assouline, and D. Or. 2008. Characteristic lengths affecting evaporative drying of porous media. Phys. Rev. E 77:056309. doi:10.1103/PhysRevE.77.056309

Lehmann, E.H., and W. Wagner. 2010. Neutron imaging at PSI: A promising tool in materials science and technology. Appl. Phys. A: Mater. Sci. Process. 99:627–634. doi:10.1007/s00339-010-5606-3

Lieleg, O., M. Caldara, R. Baumgärtel, and K. Ribbeck. 2011. Mechanical robustness of *Pseudomonasaeruginosa* biofilms. Soft Matter 7:3307–3314. doi:10.1039/c0sm01467b

Marone, F., A. Studer, H. Billich, L. Sala, and M. Stampanoni. 2017. Towards on-the-fly data post-processing for real-time tomographic imaging at TOMCAT. Adv. Struct. Chem. Imaging 3:1. doi:10.1186/s40679-016-0035-9

McCully, M.E., and J.S. Boyer. 1997. The expansion of maize root-cap mucilage during hydration: 3. Changes in water potential and water content. Physiol. Plant. 99:169–177. doi:10.1111/j.1399-3054.1997.tb03445.x

Moradi, A.B., A. Carminati, D. Vetterlein, P. Vontobel, E. Lehmann, U. Weller, et al. 2011. Three-dimensional visualization and quantifica-

tion of water content in the rhizosphere. New Phytol. 192:653–663. doi:10.1111/j.1469-8137.2011.03826.x

Naveed, M., L.K. Brown, A.C. Raffan, T.S. George, A.G. Bengough, T. Roose, et al. 2017. Plant exudates may stabilize or weaken soil depending on species, origin and time: Effect of plant exudates on rhizosphere formation. Eur. J. Soil Sci. 68:806–816. doi:10.1111/ejss.12487

Naveed, M., L.K. Brown, A.C. Raffan, T.S. George, A.G. Bengough, T. Roose, et al. 2018. Rhizosphere-scale quantification of hydraulic and mechanical properties of soil impacted by root and seed exudates. Vadose Zone J. 17:170083. doi:10.2136/vzj2017.04.0083

Ohnesorge, W.V. 1936. Die bildung von tropfen an düsen und die auflösung flüssiger strahlen. Z. Angew. Math. Mech. 16:355–358. doi:10.1002/zamm.19360160611

Ophir, T., and D.L. Gutnick. 1994. A role for exopolysaccharides in the protection of microorganisms from desiccation. Appl. Environ. Microbiol. 60:740–745.

Or, D., S. Phutane, and A. Dechesne. 2007. Extracellular polymeric substances affecting pore-scale hydrologic conditions for bacterial activity in unsaturated soils. Vadose Zone J. 6:298–305. doi:10.2136/vzj2006.0080

Paganin, D., S.C. Mayo, T.E. Gureyev, P.R. Miller, and S.W. Wilkins. 2002. Simultaneous phase and amplitude extraction from a single defocused image of a homogeneous object. J. Microsc. 206:33–40. doi:10.1046/j.1365-2818.2002.01010.x

Peters, A., S.C. Iden, and W. Durner. 2015. Revisiting the simplified evaporation method: Identification of hydraulic functions considering vapor, film and corner flow. J. Hydrol. 527:531–542. doi:10.1016/j.jhydrol.2015.05.020

Philippot, L., J.M. Raaijmakers, P. Lemanceau, and W.H. van der Putten. 2013. Going back to the roots: The microbial ecology of the rhizosphere. Nat. Rev. Microbiol. 11:789–799. doi:10.1038/nrmicro3109

Raaijmakers, J.M., I. De Bruijn, O. Nybroe, and M. Ongena. 2010. Natural functions of lipopeptides from *Bacillus* and *Pseudomonas*: More than surfactants and antibiotics. FEMS Microbiol. Rev. 34:1037–1062. doi:10.1111/j.1574-6976.2010.00221.x

Read, D.B., A.G. Bengough, P.J. Gregory, J.W. Crawford, D. Robinson, C.M. Scrimgeour, et al. 2003. Plant roots release phospholipid surfactants that modify the physical and chemical properties of soil. New Phytol. 157:315–326. doi:10.1046/j.1469-8137.2003.00665.x

Read, D.B., and P.J. Gregory. 1997. Surface tension and viscosity of axenic maize and lupin root mucilages. New Phytol. 137:623–628. doi:10.1046/j.1469-8137.1997.00859.x

Read, D.B., P.J. Gregory, and A.E. Bell. 1999. Physical properties of axenic maize root mucilage. Plant Soil 211:87–91. doi:10.1023/A:1004403812307

Roberson, E.B., C. Chenu, and M.K. Firestone. 1993. Microstructural changes in bacterial exopolysaccharides during desiccation. Soil Biol. Biochem. 25:1299–1301. doi:10.1016/0038-0717(93)90230-9

Roberson, E.B., and M.K. Firestone. 1992. Relationship between desiccation and exopolysaccharide production in a soil *Pseudomonas* sp. Appl. Environ. Microbiol. 58:1284–1291.

Rodriguez-Caballero, E., J. Belnap, B. Büdel, P.J. Crutzen, M.O. Andreae, U. Pöschl, and B. Weber. 2018. Dryland photoautotrophic soil surface communities endangered by global change. Nat. Geosci. 11:185–189. doi:10.1038/s41561-018-0072-1

Rosenzweig, R., U. Shavit, and A. Furman. 2012. Water retention curves of biofilm-affected soils using xanthan as an analogue. Soil Sci. Soc. Am. J. 76:61–69. doi:10.2136/sssaj2011.0155

Rossi, F., G. Mugnai, and R. De Philippis. 2018. Complex role of the polymeric matrix in biological soil crusts. Plant Soil 429:19–34. doi:10.1007/s11104-017-3441-4

Sattler, R., S. Gier, J. Eggers, and C. Wagner. 2012. The final stages of capillary break-up of polymer solutions. Phys. Fluids 24:023101. doi:10.1063/1.3684750

Schindler, U., W. Durner, G. von Unold, and L. Müller. 2010. Evaporation method for measuring unsaturated hydraulic properties of soils: Extending the measurement range. Soil Sci. Soc. Am. J. 74:1071–1083. doi:10.2136/sssaj2008.0358

Segura-Campos, M.R., N. Ciau-Solís, G. Rosado-Rubio, L. Chel-Guerrero, and D. Betancur-Ancona. 2014. Chemical and functional properties of chia seed (*Salvia hispanica* L.) gum. Int. J. Food Sci. 2014:241053. doi:10.1155/2014/241053

Shaw, T., M. Winston, C.J. Rupp, I. Klapper, and P. Stoodley. 2004. Commonality of elastic relaxation times in biofilms. Phys. Rev. Lett. 93:098102. doi:10.1103/PhysRevLett.93.098102

Stampanoni, M., A. Groso, A. Isenegger, G. Mikuljan, Q. Chen, A. Bertrand, et al. 2006. Trends in synchrotron-based tomographic imaging: The SLS experience. In: U. Bonse, editor, Developments in X-ray tomography V: SPIE Optics + Photonics, San Diego, CA. 13–17 Aug. 2006. Proceedings Vol. 6318. SPIE, Bellingham, WA. Pap. 63180M. doi:10.1117/12.679497

Stoodley, P., R. Cargo, C.J. Rupp, S. Wilson, and I. Klapper. 2002. Biofilm material properties as related to shear-induced deformation and detachment phenomena. J. Ind. Microbiol. Biotechnol. 29:361–367. doi:10.1038/sj.jim.7000282

The MathWorks. 2017. MATLAB. Version 9.3.0 (R2017b). The MathWorks, Natick, MA.

Volk, E., S.C. Iden, A. Furman, W. Durner, and R. Rosenzweig. 2016. Biofilm effect on soil hydraulic properties: Experimental investigation using soil-grown real biofilm. Water Resour. Res. 52:5813–5828. doi:10.1002/2016WR018866

Wloka, M., H. Rehage, H.-C. Flemming, and J. Wingender. 2004. Rheological properties of viscoelastic biofilm extracellular polymeric substances and comparison to the behavior of calcium alginate gels. Colloid Polym. Sci. 282:1067–1076. doi:10.1007/s00396-003-1033-8

Zheng, W., S. Zeng, H. Bais, J.M. LaManna, D.S. Hussey, D.L. Jacobson, and Y. Jin. 2018. Plant growth-promoting rhizobacteria (PGPR) reduce evaporation and increase soil water retention. Water Resour. Res. doi:10.1029/2018WR022656

Zickenrott, I.-M., S.K. Woche, J. Bachmann, M.A. Ahmed, and D. Vetterlein. 2016. An efficient method for the collection of root mucilage from different plant species-A case study on the effect of mucilage on soil water repellency. J. Plant Nutr. Soil Sci. 179:294–302. doi:10.1002/jpln.201500511